npj | science of food

Article

Published in partnership with Beijing Technology and Business University & International Union of Food Science and Technology

https://doi.org/10.1038/s41538-025-00662-x

Ultrasound-high pressure combined treatment effects on structure and physicochemical properties of soybean protein isolate

Jinying Li[1,2,5], Jiannan Yan[1,2,5] ✉, Fangxiao Xing[1,2], Jianjiang Wei[3], Qiyong Feng[4], Qianqian Gu[1,2], Jiale Gao[1,2], Chengbin Zhao[1,2] ✉ & Jingsheng Liu[1,2] ✉

Effects of combined ultrasound and high-pressure treatment on the structure and physicochemical properties of soybean protein isolate (SPI) were explored using infrared and fluorescence spectroscopy, an assay kit, and texture profile analysis. The combined treatment of ultrasound and high pressure resulted in the transformation of the secondary structure from order to disorder and a looser tertiary conformation. The ultrasound, followed by high-pressure treatment, resulted in a more significant unfolding of SPI structure, and further increased the thermal stability and surface charges, while reducing the average particle size. The surface hydrophobicity, free sulfhydryl groups, and solubility of SPI treated with 480 W ultrasound followed by high pressure were enhanced by 1.98 times, 47.74% and 1.42 times, respectively. Meanwhile, both emulsification and gelation properties reached the optimal levels. Modified SPI can be used as a processing raw material to apply in the design and development of high-stability emulsions or high-strength gels.

Soybean protein isolate (SPI) is an important by-product of the soybean oil industry, containing at least 90% protein. SPI, as a high-quality plant protein resource, has become a good substitute for animal protein due to its low cost, high nutritional value, and excellent functional properties such as emulsification and gelation, which are widely used in various food formulas[1]. The main component of SPI is storage protein, which is composed of glycinin (11S) and β-conglycinin (7S), accounting for approximately 70% of the total protein content. 11S is a hexamer formed by six subunits, each of which is formed by the connection of an acidic polypeptide (A, approximately 38 kDa) and a basic polypeptide (B, approximately 20 kDa) through disulfide bonds. 7S is a trimery-structured protein, mainly consisting of the α subunit (approximately 68 kDa), the α' subunit (approximately 72 kDa), and the β-subunit (approximately 52 kDa)[2]. The physicochemical properties of 11S and 7S are different due to their structural differences, which in turn affect their functions. The spatial structures of proteins, such as secondary, tertiary, and quaternary structures, determine the physicochemical properties of proteins. Moreover, the physicochemical properties of proteins are also affected by their composition, denaturation, and degree of aggregation. According to the different physicochemical properties of SPI, such as solubility, dispersibility, viscosity, emulsification, and gelation, its application forms in specific foods are also varied[3]. Wang et al.[4] also reported that the particle size, charge, surface hydrophobicity, and free sulfhydryl content of proteins all affect their solubility, interfacial properties, and gel performance. At present, the main method for preparing SPI is the alkali extraction and acid precipitation. During the preparation process, proteins are exposed to extreme conditions such as strong acids, strong bases, and high temperatures, which leads to the destruction of protein structures, thereby reducing their physicochemical properties. At present, the methods for improving the physicochemical properties of proteins mainly involve physical, chemical, and enzymatic modifications[5]. Non-thermal physical modification techniques, like ultrasound, high-pressure processing, cold plasma, and pulsed electric field, show a greater potential for application in protein modification[6].

In recent years, low-frequency high-intensity ultrasound (16-100 kHz, 10-1000 W/cm^2) has been widely used in food processing, especially in protein structure modification. The effects of ultrasound on proteins are

[1]College of Food Science and Engineering, Jilin Agricultural University, Changchun, Jilin, China. [2]National Engineering Research Center for Wheat and Corn Deep Processing, Changchun, Jilin, China. [3]College of Agriculture, Jilin Agricultural University, Changchun, Jilin, China. [4]Jilin City Laoyeling Agricultural Development Company Limited, Jilin, Jilin, China. [5]These authors contributed equally: Jinying Li, Jiannan Yan. ✉e-mail: yanjiannan91@163.com; zhaochengbin1987@163.com; liujingsheng@jlau.edu.cn

mainly related to cavitation, mechanical vibration, shear stress, and turbulence[7]. Ultrasound, as a non-thermal physical processing technology, can improve the physicochemical properties of protein aggregates by altering their spatial structure. Zheng et al.[8] found that ultrasound changed the secondary and tertiary structures of SPI, reduced the particle size, and increased the solubility, which improved the surface hydrophobicity and gelation properties of the protein. In order to further enhance the effect of ultrasonic treatment, ultrasound can be combined with other treatments to exert a synergistic effect. Shi et al.[9] demonstrated that the combined treatment of ultrasound and high-pressure homogenization improved the physicochemical, interfacial, and gel properties of whey proteins more effectively than ultrasound or high-pressure homogenization alone. Ye, Wang, Ma, and Ma[10] found that the dual modification of ultrasound and glycosylation improved the emulsification characteristics of canola protein, which reduced the particle size of the emulsion and enhanced the emulsion stability.

High-pressure treatment is also a physical modification method for food proteins. The treatment pressure is within the range of 0-1000 MPa, which can achieve the modification of protein structure and improvement of physicochemical properties under non-thermal conditions[11]. The modification of proteins by high pressure largely depends on the intensity and time of the applied pressure, as well as the type of protein, pH, and ionic strength. High pressure can alter the secondary and tertiary structures of proteins, causing the unfolding of protein molecules and the exposure of active groups buried within the molecules, which thereby improves the physicochemical properties of proteins such as emulsification and gelation[12]. Yu et al.[13] found that high-pressure treatment increased the surface hydrophobicity, α-helix, and β-turn of whey protein, facilitating the improvement of emulsion stability. The combined application of high pressure and other modification methods can further improve the physicochemical properties of proteins. Yildiz[14] improved the solubility, surface hydrophobicity, free sulfhydryl group, and emulsifying property of melon seed protein by using high pressure combined with pH shift. Qin, Shuang, and Bao[15] reported that high-pressure-assisted enzymolysis increased the flexibility of the secondary structure of sunflower meal protein, enhancing the sulfhydryl content, surface hydrophobicity, and zeta potential and reducing the molecular weight and particle size, which improved its functional properties and in vitro digestibility. It was worth noting that there were few studies on SPI treated by the combination of ultrasound and high pressure. At present, only our previous studies have reported the improvement effect of ultrasound-high-pressure combined treatment on the structure of TGase-induced SPI cold gel and its delivery for riboflavin[16,17]. However, the influence of combined ultrasound-high-pressure treatment on the structure and physicochemical properties of SPI remains unclear.

In this study, SPI was treated with combined ultrasound at different power levels and high pressure. The subunits, secondary structure, tertiary conformation, and thermal stability of the protein were characterized. The particle size, potential, surface hydrophobicity, free sulfhydryl groups, solubility, emulsification, and gelation were analyzed. The effects of ultrasound and high-pressure combined treatment on the structure and physicochemical properties of SPI were investigated, and the structure-function relationship was explored to provide a theoretical basis for the application of ultrasound-high-pressure combined processing technology in the modification of food proteins.

Results and discussion

Sodium dodecyl sulfate-polyacrylamide gel electrophoresis (SDS-PAGE)

Figure 1 shows the SDS-PAGE of SPI treated with combined ultrasound and high pressure. SPI was mainly composed of the acidic (A) and basic (B) subunits of glycinin (11S) as well as the α, α', and β subunits of β-conglycinin (7S)[16]. The ultrasound-high-pressure combined treatment did not change the composition and distribution of SPI subunits, indicating that the protein did not degrade and its primary structure was not damaged. Similar results

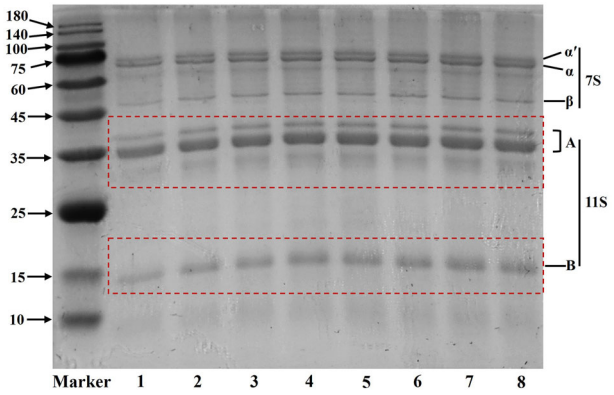

Fig. 1 | Sodium dodecyl sulfate-polyacrylamide gel electrophoresis of soybean protein isolate treated with combined ultrasound and high pressure. Lane 1: Control; Lane 2: HP; Lane 3: U240; Lane 4: HP-U240; Lane 5: U240-HP; Lane 6: U480; Lane 7: HP-U480; Lane 8: U480-HP.

were also found in the research of black bean protein[18] and pea protein[19]. However, different ultrasound conditions and their combination sequence with high pressure all increased the intensity of SPI subunit bands, especially the low molecular weight subunits. It was possible that ultrasound and high pressure promoted the breakage of protein disulfide bonds, forming more low molecular weight subunits[20]. There was no significant difference in the intensity of SPI subunit bands under all the ultrasound-high-pressure combined treatment conditions. The results were consistent with those reported by previous researchers, who found that ultrasound[21] and high pressure[12] treatments did not change the distribution of protein subunits, but enhanced the intensity of subunit bands.

Fourier transform infrared spectroscopy (FTIR)

The FTIR spectra of SPI samples treated with combined ultrasound and high pressure are shown in Fig. 2A. Different ultrasound powers and their combination sequence with high pressure did not affect the intensity of the absorption peak of SPI, but changed the position of the absorption peak. SPI had typical amide band absorption peaks at 1657 cm^{-1} (amide I), 1543 cm^{-1} (amide II), and 1240 cm^{-1} (amide III), corresponding to C = O stretching vibration, N-H bending vibration, and C-N stretching vibration, respectively[22]. The ultrasound-high-pressure combined treatment did not cause the amide I band of SPI to shift. Both the 240 W ultrasound followed by high-pressure treatment and the combined treatment of 480 W ultrasound and high-pressure resulted in the shift of the absorption peaks of amide II and amide III bands to 1545 and 1242 cm^{-1}, respectively. The absorption peak at 2929 cm^{-1} was generated by the C-H stretching vibration of CH_3 and CH_2 groups[23]. Ultrasound or high-pressure treatment alone did not affect the position of the absorption peak, but ultrasound and high-pressure combined treatment led to the shift of C-H absorption peak to 2931 cm^{-1}. Strong, wide peaks appeared at 3200-3600 cm^{-1}, which were attributed to the -OH stretching vibration[24]. Ultrasound or high pressure alone and the combination of both treatments all shifted the -OH absorption peak of SPI from 3294 cm^{-1} to 3298 cm^{-1}, suggesting the changes in intermolecular or intramolecular hydrogen bonds[25]. The absorption peaks of SPI with different treatments at 1080 cm^{-1} and 700 cm^{-1} did not change significantly, which did not lead to the conversion or destruction of NH_2. The changes of these absorption peaks indicated that the ultrasound-high-pressure combined treatment did not degrade protein, but it led to changes in the spatial structure of protein.

The amide I band of FTIR (1600–1700 cm^{-1}) can reflect the secondary structure of proteins. Gaussian peak fitting was performed on the amide I band. The corresponding relationships between each sub-peak and the secondary structure in the fitted spectra were as follows: 1610–1640 cm^{-1}, 1640–1650 cm^{-1}, 1650–1660 cm^{-1}, and 1660–1700 cm^{-1} correspond to β-sheet, random coil, α-helix, and β-turn, respectively[26]. The content of each

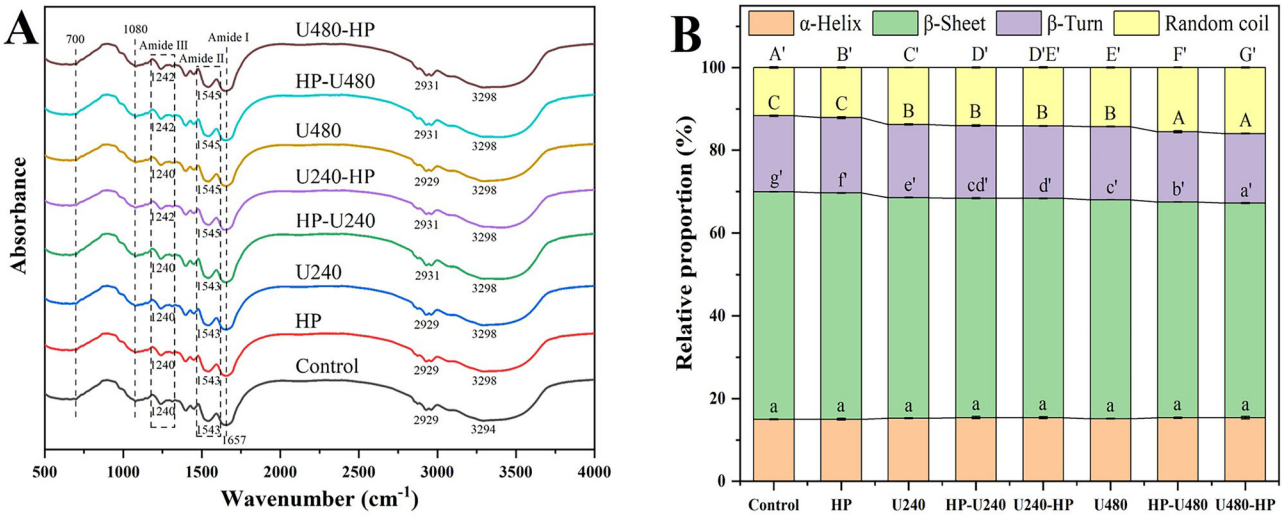

Fig. 2 | Functional groups and secondary structure of soybean protein isolate treated with combined ultrasound and high pressure. A Fourier transform infrared spectra; **B** Secondary structure contents. The different lowercase or uppercase letters in the graphs indicate that the results are significantly different ($p < 0.05$).

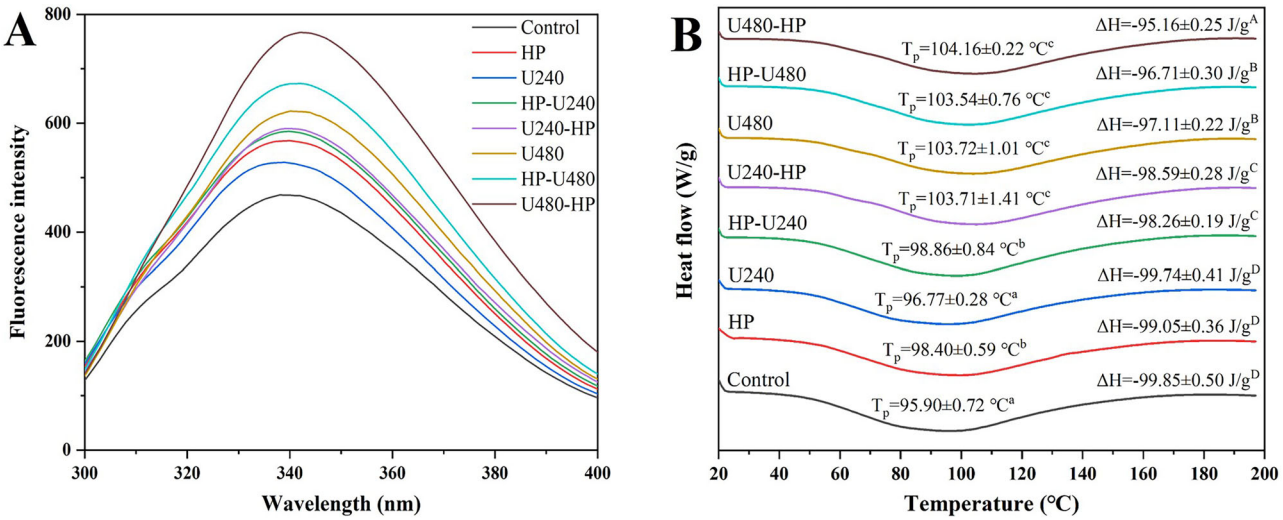

Fig. 3 | Tertiary conformation and thermal properties of soybean protein isolate treated with combined ultrasound and high pressure. A Intrinsic fluorescence spectra; **B** Differential scanning calorimetry thermograms.

secondary structure was calculated based on the peak area, and the results are shown in Fig. 2B. There was no significant difference in α-helix of SPI with different treatments. Compared with the untreated SPI, SPI treated with high pressure alone had lower β-sheet, higher random coil, and similar β-turn. The ultrasound alone and ultrasound-high-pressure combined treatment further reduced β-sheet and β-turn, increased random coil, promoting the transformation of β-structure into random coil, which resulted in the disorder of SPI secondary structure. This transformation of the secondary structure was more significant at a higher ultrasonic power (480 W), and the disorder degree of U480-HP was greater than that of HP-U480. This change in the secondary structure might be related to the disruption of intermolecular or intramolecular hydrogen bonds of protein (Fig. 2A). The ultrasound-high-pressure combined treatment induced a certain degree of unfolding of SPI molecules, transforming the secondary structure from order to disorder, resulting in an increase of molecular flexibility, which might be beneficial to the improvement of its functional properties[27].

Intrinsic fluorescence spectroscopy

Intrinsic fluorescence spectra are mainly attributed to tryptophan, tyrosine, and phenylalanine residues. Among them, tryptophan residues are more sensitive to solvent polarity. Therefore, the fluorescence quantum yield of tryptophan can be used to identify structural changes of proteins[28]. Figure 3A shows the intrinsic fluorescence spectra of SPI treated with combined ultrasound and high pressure. When the fluorescence emission maximum wavelength (λ_{max}) was less than 330 nm, tryptophan was considered to be in a non-polar environment; On the contrary, tryptophan was in a polar environment when $\lambda_{max} > 330$ nm[29]. The λ_{max} of all samples was greater than 330 nm, indicating that tryptophan residues were all present in the polar environment. The λ_{max} of untreated SPI was 338 nm, and the λ_{max} of U240 was 339 nm. The λ_{max} of HP, HP-U240, U240-HP, and U480 was 340 nm, and the λ_{max} of HP-U480 and U480-HP was 342 nm. The ultrasound-high-pressure combined treatment caused various degrees of redshift (towards longer wavelengths) in the λ_{max} of SPI, which suggested that the protein structure tended to be exposed and the tryptophan residues were exposed to a more hydrophilic polar environment[30]. A more polar microenvironment of tryptophan residues meant that a looser tertiary conformation of proteins[8]. In addition, ultrasound, high pressure, and their combination treatment all increased the fluorescence intensity of SPI. The fluorescence intensity of the samples treated with high power (480 W) ultrasound combined with high pressure was enhanced more significantly, and U480-HP exhibited the maximum fluorescence intensity. This might be due to the fact that the ultrasound-high-pressure combined treatment

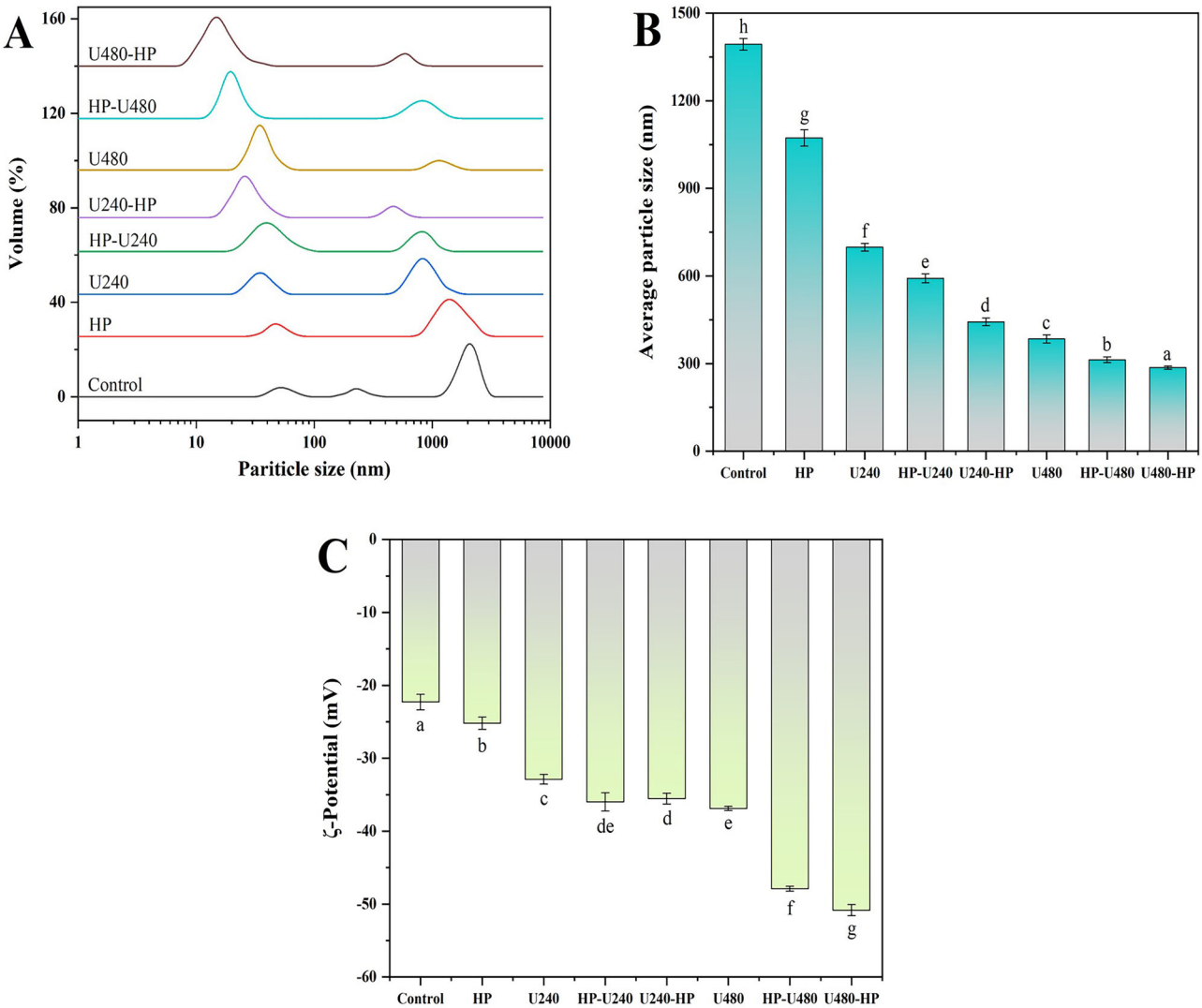

Fig. 4 | Aggregation and dispersion of soybean protein isolate treated with combined ultrasound and high pressure. A Particle size distribution; **B** Average particle size; **C** ζ-potential. The different letters in the graphs indicate that the results are significantly different ($p < 0.05$).

promoted the unfolding of protein structure, resulting in the exposure of more tryptophan residues[31]. The increase in ultraviolet (UV) absorption intensity indicated that the combined ultrasound and high-pressure treatment of SPI resulted in the exposure of aromatic amino acid residues and a more unfolded structure of protein (Fig. S1), which also supported the results of fluorescence analysis. The looser tertiary conformation and more exposed structure of SPI also implied an increase in structural flexibility, which might enhance its functional properties such as emulsification and gelation.

Differential scanning calorimetry (DSC)

The energy changes and thermal properties during the protein denaturation process can be characterized by DSC[32]. The DSC thermograms of SPI treated with combined ultrasound and high pressure are shown in Fig. 3B. SPI only showed a single endothermic peak of glycinin (11S) at around 100 °C, but no endothermic peak of β-conglycinin (7S), due to the denaturation of 7S in commercial SPI. The peak temperature (T_p) is the denaturation temperature of the protein, which is related to its thermal stability[33]. Compared with the untreated SPI, the T_p of samples treated with ultrasound or high pressure alone increased, and the T_p of the sample treated with 480 W ultrasound was even higher. U240-HP exhibited a higher T_p compared to samples subjected to the individual treatments, while the combination of ultrasound and high pressure did not further increase T_p at a higher power of 480 W. The ultrasound and high pressure unfolded the protein structure, exposing the active groups and promoting the intermolecular interactions of the protein, which thereby improved the thermal stability[34]. The enthalpy change (ΔH) reflects the denaturation degree and conformational change of protein[35]. Neither 240 W ultrasound nor high pressure alone affected the ΔH of SPI, while 480 W ultrasound treatment of SPI reduced the ΔH. The ultrasound-high-pressure combined treatment further reduced the ΔH of SPI, and the ΔH of U480-HP sample was the lowest, which might be related to the folding and aggregation state of SPI[36]. Furthermore, the decrease in ΔH might also be attributed to the loss of partially ordered protein structures, such as β-structure (Fig. 2B). The decrease in ΔH indicated that the ultrasound-high-pressure combined treatment caused partial denaturation of SPI, resulting in a looser tertiary conformation, which was supported by the changes of the intrinsic fluorescence spectra (Fig. 3A).

Particle size

The particle size of protein is one of the factors affecting its functional properties, characterizing the aggregation degree of protein[37]. Figure 4A shows the particle size distribution of SPI treated with ultrasound-high-pressure combined treatment. The untreated SPI showed a multi-peak particle size distribution, which was distributed at 10–100 nm, 100–1000 nm, and 1000–10,000 nm, exhibiting the greatest distribution at

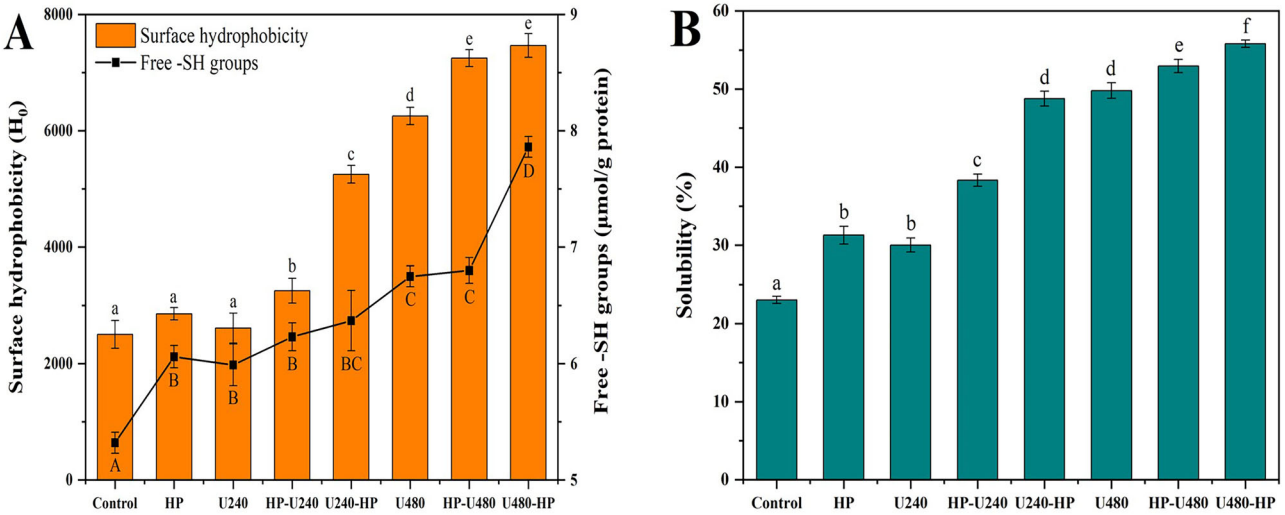

Fig. 5 | Surface properties and solubility of soybean protein isolate treated with combined ultrasound and high pressure. A Surface hydrophobicity and free sulfhydryl groups; **B** Solubility. The different lowercase or uppercase letters in the graphs indicate that the results are significantly different ($p < 0.05$).

1000–10,000 nm. The particle size distribution peak of the HP sample moved towards a smaller particle size, and the distribution peak at 100–1000 nm disappeared. The distribution peaks of the samples treated by 240 W ultrasound and its combined treatment with high pressure shifted more significantly to smaller particle sizes, and the samples treated by the combined treatment of ultrasound and high pressure had a greater distribution at 10–100 nm. Although the samples treated by 480 W ultrasound and its combined treatment with high pressure had a relatively small shift of the small distribution peaks at 1000–10,000 nm, the large distribution peaks at 10–100 nm moved more towards the smaller particle size, especially U480-HP had more distribution within a smaller particle size range.

Figure 4 B shows the average particle size of SPI treated with combined ultrasound and high pressure. Compared with the untreated SPI, the average particle size of SPI after ultrasound or high-pressure treatment was significantly reduced. The average particle size of the control was 1393 nm, while that of HP was decreased to 1073 nm, indicating that high-pressure treatment of protein led to the destruction of large aggregates and the formation of smaller aggregates[38]. The average particle sizes of U240 and U480 were reduced to 698 and 384 nm, respectively. It was possible that the cavitation and microstreaming effect induced by ultrasound interfered with the intermolecular interactions of proteins, dissociating the aggregates of SPI[39]. Furthermore, the samples treated with combined ultrasound and high pressure had a smaller particle size than the samples treated alone, which was attributed to a synergistic effect of ultrasound and high pressure, causing a less compact structure of protein and promoting the formation of smaller-sized protein particles[40]. Whether it was 240 W or 480 W, the particle size of samples treated with ultrasound followed by high pressure was lower than that of the samples treated in the reverse order, which was the lowest for U480-HP (286 nm). Both the ultrasound power and the sequence of ultrasound-high-pressure combined treatment affected the changes in particle size of SPI.

ζ-potential

Figure 4C shows the ζ-potential of SPI treated with combined ultrasound and high pressure. The ζ-potentials of all SPI samples were negative, suggesting that the SPI surface had more negatively charged amino acids[18]. A higher ζ-potential absolute value indicated that the electrostatic repulsion on the protein surface was greater, and the stability of protein dispersion was enhanced[41]. Compared with the untreated sample, the surface charges of samples treated with ultrasound or high pressure alone were increased, and the ultrasound-high pressure combined treatment further increased the surface charges. At low power (240 W), the treatment sequence of ultrasound and high pressure did not affect the ζ-potential of the protein. At high power (480 W), the surface charge of the sample (U480-HP) treated with ultrasound, followed by high pressure, was the highest. It was possible that ultrasound-high-pressure combined treatment unfolded the protein structure (Fig. 2 and Fig. 3), leading to more negatively charged amino acid groups being exposed on the molecular surface. The increase in negative charges on the protein surface induced by the combination of ultrasound and high pressure promoted the electrostatic repulsion between protein particles, which inhibited protein aggregation and prevented the formation of large-sized aggregates, thereby forming smaller particle sizes and improving the stability of protein dispersions[42]. This also confirmed that the combined ultrasound and high pressure resulted in a reduction in particle size of SPI (Fig. 4B).

Surface hydrophobicity (H_0)

The H_0 of protein reflects the number of exposed hydrophobic groups. The H_0 of SPI treated with combined ultrasound and high pressure is shown in Fig. 5A. Compared with the untreated SPI, there was no significant change in H_0 of HP and U240 samples, while the H_0 of U480 increased significantly. It indicated that the cavitation caused by high-intensity ultrasound had a stronger effect on the unfolding of protein structure and the exposure of hydrophobic groups[43]. This was consistent with the increase in H_0 of pea protein induced by ultrasound[44]. Furthermore, the ultrasound-high-pressure combined treatment further increased the H_0 of SPI. At an ultrasonic power of 240 W, the H_0 of U240-HP was higher than that of HP-U240. At an ultrasonic power of 480 W, the combined effect of ultrasound and high pressure on the improvement of H_0 was more significant, but the treatment sequence of ultrasound and high pressure did not affect H_0. The H_0 of the U480-HP sample was 1.98 times higher than that of the untreated SPI. The combined treatment of SPI by high-power ultrasound (480 W) and high pressure reduced the β-structure (β-sheet and β-turn) and formed a more extended structure, which promoted the exposure of hydrophobic groups inside the protein on the molecular surface and provided more binding sites for ANS fluorescent probes, resulting in a higher H_0[40].

Free sulfhydryl (-SH) groups

Free -SH groups are those located on the surface of proteins, reflecting the unfolding degree of protein structure. The free -SH contents of SPI treated with combined ultrasound and high pressure are shown in Fig. 5A. Compared with the untreated SPI, the free -SH contents of samples treated by ultrasound or high pressure alone and their combination increased significantly, indicating that both ultrasound and high pressure could unfold the SPI molecules and expose the originally buried -SH groups. Similar results were also found in the studies of SPI treated by ultrasound[45] and

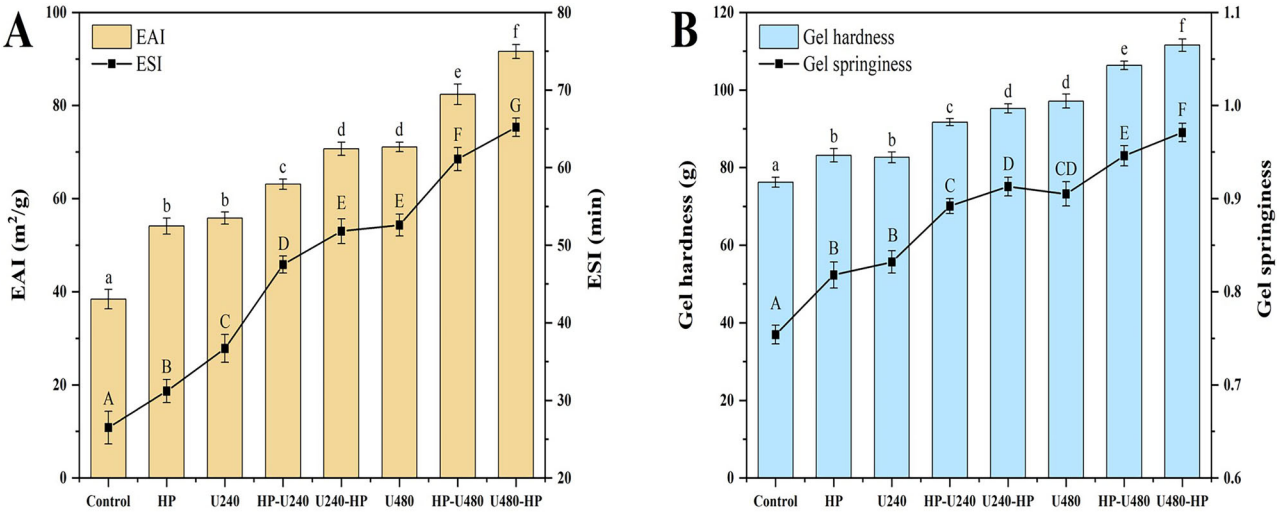

Fig. 6 | Functional properties of soybean protein isolate treated with combined ultrasound and high pressure. A Emulsifying properties; **B** Gelation properties. The different lowercase or uppercase letters in the graphs indicate that the results are significantly different ($p < 0.05$).

myofibrillar protein treated by high pressure[46]. At low ultrasonic power (240 W), there was no significant difference between the ultrasound-high-pressure combined treatment and the separate treatment. Individual 480 W ultrasound and its combination with high pressure further increased the free-SH content of SPI, and the free-SH of U480-HP reached the highest level, which was 47.74% higher than the untreated SPI, proving the synergistic promoting effect of high-power ultrasound and high pressure on the unfolding of SPI. Furthermore, ultrasound-high-pressure combined treatment might disrupt partial disulfide bonds of SPI molecules, resulting in an increase of free -SH groups[47], which also explained the reason for the lowest particle size of U480-HP (Fig. 4B).

Solubility

Solubility is a commonly used method for measuring protein denaturation and aggregation, and it plays a crucial role in other functional properties of proteins, such as emulsification and gelation. The solubility of SPI treated with combined ultrasonic and high pressure is shown in Fig. 5B. All treatments promoted the solubility of SPI. There was no significant difference in solubility between HP and U240 samples, while the U480 sample had a higher solubility. The combined treatment of ultrasound and high pressure further improved the solubility of SPI, and the solubility of samples treated with ultrasound followed by high pressure was higher than that of samples treated in the reverse order. The solubility of the U480-HP sample (55.80%) reached the highest level, which was approximately 1.42 times higher than that of the untreated SPI (23.02%). The increase in solubility might be due to the fact that the ultrasound-high-pressure combined treatment partially unfolded the protein molecules, exposing more polar groups, which enhanced the interactions between protein and water[48]. Sun et al.[49] found that the increase in solubility was related to the changes in the three-dimensional structure of globular proteins. A more disordered secondary structure (Fig. 2) and a looser tertiary conformation (Fig. 3) improved the flexibility of SPI molecules, thereby increasing their solubility. Furthermore, the improvement in the solubility of SPI under ultrasound-high pressure combined treatment was also associated with its smaller particle size (Fig. 4A, B) and higher surface charge (Fig. 4C). High surface charge enhanced the electrostatic repulsion between protein particles, inhibited protein aggregation or precipitation and formed small-sized soluble protein aggregates, leading to an increase in protein solubility, which was supported by the results of Zhou et al.[50]. However, the solubility of both untreated and treated SPI in this work were lower than those determined using the biuret method by Dehnad et al.[51], who treated SPI with 400 MPa high pressure for 15 min. This might be related to shorter high-pressure time (5 min) in this work. In addition, solubility was determined using the BCA method rather than the biuret method in this work, which might also lead to differences in solubility. It was worth noting that the combined treatment of ultrasound and high pressure improved both the H_0 and solubility of SPI, which was related to the reduced β-structure and higher unfolding degree of protein. This change increased the exposure of hydrophobic and polar groups, promoting protein-water interactions, which contributed to the development of functional properties of proteins, such as emulsification and gelation[12].

Emulsifying properties

Figure 6A shows the emulsifying properties of SPI treated with combined ultrasound and high pressure. Compared with untreated SPI, ultrasound or high pressure alone improved the EAI and ESI of SPI, and high-power (480 W) ultrasound had a more significant improvement effect. The EAI and ESI of the samples treated with combined ultrasound and high pressure further increased. The SPI treated with ultrasound followed by high pressure exhibited more excellent emulsifying properties than that treated in the reverse order at the same ultrasonic power, and the U480-HP had the highest EAI and ESI. The change trend in creaming index (CI) of all samples was consistent with that of ESI, and the U480-HP showed the lowest CI (Fig. S2), which also supported its highest ESI. The ultrasound-high-pressure combined treatment enabled protein to unfold to a greater extent, leading to a more disordered (Fig. 2) and less compact (Fig. 3) structure, exposing the buried hydrophobic groups (Fig. 5A), which thus promoted protein dissolution (Fig. 5B). This structural modification and high amphiphilicity facilitated the adsorption of proteins at the oil-water interface and reduced the interfacial tension, which improved the emulsification ability of proteins[52]. Furthermore, lower particle size (Fig. 4A, B) and higher surface charge (Fig. 4C) were conducive to the structural rearrangement and interaction of interface proteins, preventing their aggregation by increasing the electrostatic repulsion and steric hindrance between emulsified droplets, which thereby promoted the formation of emulsions and improved their stability[53]. Hegde et al.[54] also found that the combination of ultrasound and high pressure improved the emulsification properties of pearl millet protein, which was in agreement with the results of this study.

Gelation properties

Figure 6B shows the gelation properties of SPI treated with combined ultrasound and high pressure. The gel hardness and gel springiness of the samples treated differently were improved to varying degrees. There was no significant difference in the gel texture characteristics between HP and U240 samples, while the gel hardness and springiness of the U480 sample further increased. Compared with the untreated SPI (76.24 g), the gel hardness of

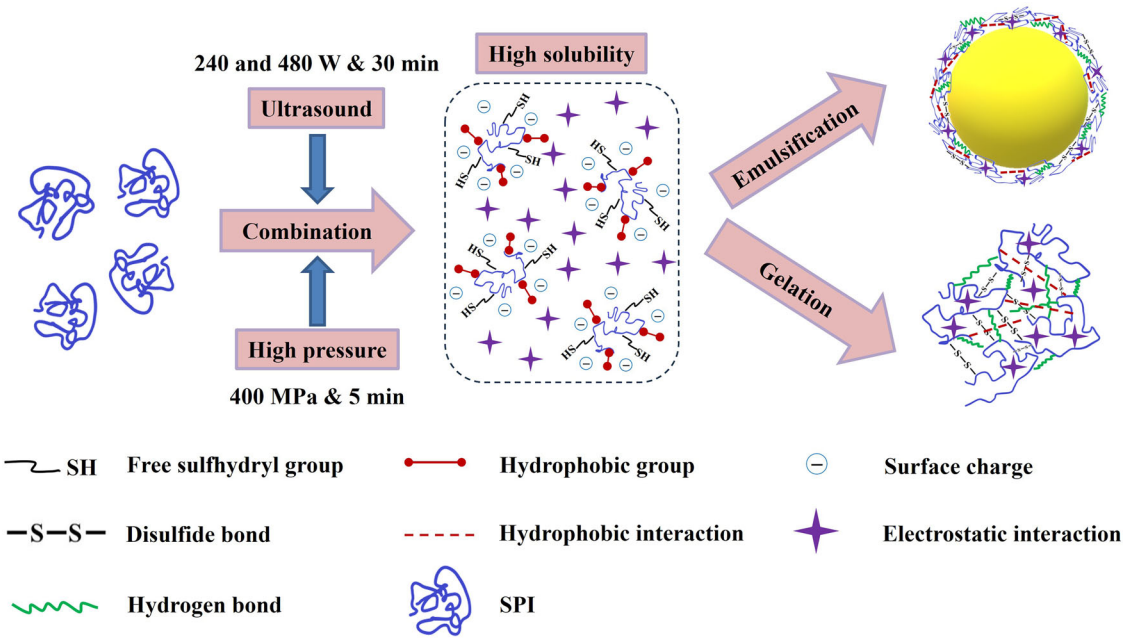

Fig. 7 | Proposed mechanism for the effect of combined ultrasound and high pressure on the physicochemical properties of soybean protein isolate.

HP (83.17 g), U480 (97.14 g), HP-U480 (106.35 g), and U480-HP (111.54 g) increased by 9.09%, 27.41%, 39.49% and 46.30%, respectively. Previous reports also showed that both ultrasound[8] and high pressure[20] enhanced the gelation properties of plant proteins by altering their secondary structure and tertiary conformation, which were in agreement with the results of this work. The improvement effect of gel hardness by ultrasound-high-pressure combined treatment was greater than the sum of the enhancement of gel hardness by ultrasound or high pressure alone. The variation trend of gel springiness was similar to that of gel hardness, indicating a synergistic improvement in SPI gel texture by ultrasound and high pressure. The samples treated with ultrasound followed by high pressure exhibited higher gel hardness and springiness than those treated in the reverse order. The ultrasound and high-pressure combined treatment modified the secondary (Fig. 2) and tertiary structures (Fig. 3) of proteins, and increased H_0 and free -SH groups (Fig. 5A), which promoted the aggregation and cross-linking between protein molecules through hydrophobic interactions and disulfide bonds during the heat treatment process, resulting in the improvement of gel texture properties[55]. Furthermore, the gelation properties of protein were also enhanced by changing its particle size and charge distribution (Fig. 4) as well as the solubility (Fig. 5B)[56]. The U480-HP sample had the highest gel hardness and springiness. Therefore, 480 W ultrasound followed by high-pressure treatment can be used for the development of high-strength protein gels.

Proposed mechanism

The proposed mechanism for the effect of combined ultrasound and high pressure on physicochemical properties of SPI is shown in Fig. 7. The combination of ultrasound and high pressure caused partial denaturation and structural unfolding of SPI, transforming the secondary structure from order to disorder and forming a less compact tertiary conformation. This change of protein structure reduced the particle size and increased the surface charges, enhancing the intermolecular electrostatic repulsion, which promoted protein-water interactions and improved the solubility of the protein. In addition, the unfolding of the SPI structure increased molecular flexibility, exposing more charged groups, hydrophobic groups, and -SH groups on the protein molecule surface, which promoted the binding and cross-linking of proteins at the oil-water interface or in water through multiple forces such as hydrogen bonds, electrostatic interactions, hydrophobic interactions, and disulfide bonds. Therefore, ultrasound-high-pressure combined treatment synergistically improved the emulsifying and gelation properties of proteins, which facilitated to formation of stable emulsions and high-strength gels.

In conclusion, the combination of ultrasound and high pressure did not change the composition and distribution of SPI subunits, but it induced the unfolding of SPI molecules, promoting the transformation of β-structure to random coil and leading to a redshift of λ_{max}, which enhanced the fluorescence intensity and T_p, and reduced ΔH. The ultrasound followed by high-pressure treatment of SPI further reduced the average particle size and increased the surface charge, which also resulted in the improvements in H_0, free -SH groups, solubility, emulsifying properties, and gelation behavior. U480-HP showed an increase of 1.98 times in H_0, 47.74% in free -SH groups, and 1.42 times in solubility, and both the emulsifying and gelling properties reached the optimal level. Therefore, the physicochemical properties of SPI can be effectively improved by regulating the ultrasonic power and its combination sequence with high pressure. This study can provide new insights for the optimization of the combination mode of ultrasound and high pressure and its application for improving the physicochemical properties of SPI. The SPI treated by the combination of ultrasound and high pressure can be applied to the development and production of high-quality emulsion-based beverages or gel-based meat products. Nevertheless, this study only focused on the SPI structure and physicochemical properties resulting from the ultrasound-high-pressure combined treatment, without addressing the aspect of protein digestion. Furthermore, the processing environmental factors were not taken into account. In the future, it is necessary to strengthen the research on the combined treated SPI digestion behavior and the influence of different processing environments, such as pH and temperature, on the physicochemical properties of SPI.

Methods

Materials

Soybean protein isolate (SPI, purity of 90.6%), sodium dodecyl sulfate (SDS), β-mercaptoethanol, and 1-anilino-8-naphtalene-sulfonate (ANS) were purchased from Yuanye Biotechnology Co. Ltd. (Shanghai, China). Potassium bromide (KBr), ethylene diamine tetraacetic acid (EDTA), and 5,5′-dithiobis-(2-nitrobenzoic acid) (DTNB) were provided by Sigma-Aldrich (St Louis, MO, USA). All reagents used were of analytical grade.

SPI treated with combined ultrasound and high pressure

SPI dispersion (2%, w/v) was prepared by dispersing SPI in 0.01 M phosphate buffer (pH 7.0), and stirring for 2 h at room temperature, then fully hydrated in a refrigerator at 4 °C for 24 h. An ultrasonicator (JY92-IIN, Ningbo Scientz Biotechnology Co. Ltd., Ningbo, Zhejiang, China) with a frequency of 20 Hz was used to treat the protein dispersion. The output power was set to 240 or 480 W, and treatment time was 30 min with a mode of pulse durations of 2 s on and 4 s off[16]. The sample temperature was controlled at 20–30 °C during the entire ultrasonic process. The SPI dispersion was placed in a polyethylene bag for vacuum package heat sealing. A high-pressure processing device (BaoTou KeFa High Pressure Technology Co., Ltd., Baotou, Inner Mongolia, China) was used to treat the sample at 400 MPa for 5 min using water as the medium for pressure transfer[19]. The protein samples treated with combined ultrasound and high pressure were freeze-dried. The samples treated with ultrasound followed by high pressure were labeled U240-HP and U480-HP, which were treated with high pressure and ultrasound successively were recorded as HP-U240 and HP-U480. The ultrasonically treated SPI were denoted as U240 and U480, and SPI treated with high pressure were recorded as HP. Untreated SPI was used as the control.

Sodium dodecyl sulfate-polyacrylamide gel electrophoresis (SDS-PAGE)

The mini protean® tetra system (Bio-Rad Laboratories, California, USA) was used to perform the SDS-PAGE according to the method reported by Hu et al.[57]. The 5% stacking gel and 12% separating gel were prepared. The SPI sample (2 mg/mL) was mixed with 5× loading buffer (containing SDS and β-mercaptoethanol), and then boiled for 5 min and centrifuged at 10,000 g for 15 s. The loading volume was 10 μL. The voltage of the stacking gel and the separating gel was 80 V and 120 V, respectively. After electrophoresis, the gels were stained, detained, and photographed.

Fourier transform infrared spectroscopy (FTIR)

A Vertex 70 infrared spectrometer (Bruker Company, Germany) was used to measure the FTIR spectra of the protein, referring to the method of Zhao et al.[58]. The freeze-dried sample (2 mg) was mixed with dried KBr (200 mg), ground, and pressed into tablets for measurement. The wavenumber scanning range and the resolution were 500-4000 cm^{-1} and 4 cm^{-1}, respectively. The amide I bands at 1600–1700 cm^{-1} were fitted using Peakfit software to quantitatively analyze the secondary structure of the protein.

Intrinsic fluorescence spectroscopy

A Hitachi F-2000 fluorescence spectrophotometer (Hitachi, Ltd., Tokyo, Japan) was used to measure the intrinsic fluorescence spectra of SPI according to the procedure reported by Zhao et al.[59]. The SPI sample was dispersed in 0.01 M phosphate buffer solution (pH 7.0) to obtain 2 mg/mL dispersion. The excitation wavelength was 280 nm, the slit width was 5 nm, and the emission spectra were recorded within the wavelength range of 300-400 nm.

Ultraviolet (UV) spectroscopy

The SPI sample was dispersed in 0.01 M phosphate buffer (pH 7.0) to form a protein dispersion with a concentration of 0.1 mg/mL. The phosphate buffer was used as a blank. The UV spectra were recorded at the scanning wavelength range of 250-350 nm and the slit width of 5 nm.

Differential scanning calorimetry (DSC)

DSC (Q2000, TA Instruments, USA) was used to investigate thermal properties of SPI samples, referring to the method of Hu et al.[32]. Approximately 5 mg of the sample was sealed and pressed into tablets in an aluminum pan. An empty aluminum pan was used as the reference. The peak temperature (T_p) and enthalpy change (ΔH) were recorded during the temperature rising from 20 °C to 200 °C with a heating rate of 10 °C/min and a nitrogen flow rate of 50 mL/min.

Particle size and ζ-potential

The SPI sample was dissolved in deionized water to prepare a 1.0 mg/mL dispersion and stirred at room temperature for 2 h. The sample was stored at 4 °C overnight to ensure complete dissolution. A Zetasizer Nano-ZS90 (Malvern Instruments Ltd., Malvern, UK) was used to measure the particle size and ζ-potential according to the method of Tian et al.[60]. The refractive index of the solvent was 1.330, and the particle size distribution of the samples was obtained according to the Mie theory. The ζ-potential was determined using the Smoluchowski model.

Measurement of surface hydrophobicity (H_0)

Referring to the method of Wang et al.[42], the H_0 of SPI was determined using ANS as the fluorescence probe. The SPI sample was dissolved in 0.01 M phosphate buffer solution (pH 7.0) to prepare protein solutions of 0.05, 0.1, 0.2, 0.5, and 1 mg/mL, respectively. Then, 20 μL of 8.0 mM ANS solution (prepared with the same buffer) was mixed with 2 mL of sample solution. The mixture was placed in a 96-well plate, and the fluorescence intensity was measured with an excitation wavelength and emission wavelength of 390 nm and 470 nm. H_0 was represented by the initial slope of the fluorescence intensity versus protein concentration curve.

Measurement of free sulfhydryl (-SH) groups

The Ellman's reagent (DTNB) was used to measure the free -SH groups of the sample according to the method reported by Zhao et al.[61]. The SPI sample was dissolved in Tris-glycine buffer solution (0.086 M Tris, 0.09 M glycine, 4 mM EDTA; pH 8.0) to obtain the protein concentration of 2 mg/mL. The sample was shaken overnight in a water bath at 37 °C, and centrifuged at 10,000 *g* for 15 min. The supernatant (3 mL) was mixed with 0.06 mL of Ellman reagent (4 mg of DTNB per mL of buffer). The mixture was incubated at for 15 min room temperature, and the absorbance at a wavelength of 412 nm was measured. The buffer solution without SPI was used as the blank reagent. The calculation formula of free -SH groups was as follows:

$$\text{Free} - \text{SH groups}\,(\mu\text{mol/g}) = \frac{73.53 \times A_{412} \times D}{C} \quad (1)$$

where A_{412} is the absorbance at 412 nm; D is the dilution factor; C is the protein concentration (mg/mL).

Measurement of solubility

The solubility of the sample was measured based on the method of Cortés-Ríos et al.[62]. The SPI sample (2 mg/mL) was dissolved in 0.01 M phosphate buffer solution at pH 7.0. The mixture was incubated overnight in a water bath at 25 °C with continuous shaking, and then centrifuged at 10,000 *g* for 20 min. The bicinchoninic acid (BCA) protein assay kit was used to determine the soluble protein content in the supernatant. The formula for calculating the protein solubility was as follows:

$$\text{Solubility}(\%) = \frac{C_{\text{soluble}}}{C_{\text{total}}} \quad (2)$$

where C_{soluble} is the soluble protein content in the supernatant; C_{total} is the total protein content in the sample.

Measurement of emulsifying properties

The emulsifying activity index (EAI) and emulsifying stability index (ESI) of protein were measured according to the procedure of Zhao et al.[53] with some modifications. The protein samples were dissolved in 0.01 M phosphate buffer solution (pH 7.0) to make the protein mass concentration of 2 mg/mL. The protein solution was mixed with soybean oil at a volume ratio of 3:1, and then homogenized at 14,000 rpm for 3 min to obtain the emulsion. The 50 μL emulsion was taken at 0 min and 10 min, and diluted 100 times with 0.1% (w/v) sodium dodecyl sulfate (SDS) solution. The absorbance at a wavelength of 500 nm was measured. The 0.1% (w/v) SDS solution without

sample was used as a blank. The calculation formulas of EAI and ESI were as follows:

$$EAI\left(m^2/g\right) = \frac{2 \times 2.303 \times A_0 \times DF}{C \times \varphi \times \theta \times 10,000} \quad (3)$$

$$ESI(\min) = \frac{A_0}{A_0 - A_{10}} \times 10 \quad (4)$$

where DF is the dilution factor (100); C is the protein concentration (g/mL); φ is the optical path (1 cm); θ is the volume fraction (0.25) of oil phase in the emulsion; A_0 and A_{10} are the absorbances of emulsions at 0 min and 10 min, respectively.

Measurement of creaming index (CI)

The freshly prepared emulsions were injected into sample bottles sealed with glass caps, and the total heights of the emulsions were determined. The height of the supernatant was measured during storage at room temperature for 12, 24, and 36 h. The CI was calculated as follows:

$$CI(\%) = \frac{H_s}{H_t} \times 100 \quad (5)$$

where H_s was the height of the subnatant after stratification, and H_t was the total height of the emulsion.

Measurement of gel texture

The SPI sample was dispersed in 0.01 M phosphate buffer solution (pH 7.0) to prepare a 12% (w/v) protein dispersion. The dispersion was magnetically stirred for 2 h and heated at 95 °C for 20 min to form a thermally induced gel. Subsequently, the gel was immediately cooled in an ice water bath for 15 min and refrigerated at 4 °C for 24 h. The texture properties of gels were determined by using a texture analyzer (TA-XT Plus, Stable Micro Systems Co. Ltd., Surrey, UK) according to the procedure of Qi et al.[63]. The gel samples were left to stand at room temperature for 1 h before measurement. The determination was carried out using texture profile analysis (TPA) mode with a P/0.5 probe. The compression speed was set to 2 mm/s and the compression ratio was 30%. The interval between two compressions was 5 s, and the trigger force was 5 g. The gel hardness and gel springiness were recorded during the testing.

Statistical analysis

All measurements were carried out in triplicate, and the data in figures and tables were expressed as mean ± standard deviation. Significant differences were defined by $p < 0.05$, which was determined by analysis of variance using SPSS software v. 25.0 (SPSS Inc., Chicago, IL). Origin 2018 software (OriginLab Corporation, Northampton, USA) was used to draw the graphs.

Data availability

The authors declare that the data supporting the findings of this study are available within the article.

Received: 12 August 2025; Accepted: 30 November 2025;
Published online: 10 December 2025

References

1. Rout, S., Dash, P., Panda, P. K., Yang, P.-C. & Srivastav, P. P. Interaction of dairy and plant proteins for improving the emulsifying and gelation properties in food matrices: A review. *Food Sci. Biotechnol.* **33**, 3199–3212 (2024).
2. Zhang, J., Wang, J., Li, M., Guo, S. & Lv, Y. Effects of heat treatment on protein molecular structure and in vitro digestion in whole soybeans with different moisture content. *Food Res. Int.* **155**, 111115 (2022).
3. Rout, S., & Srivastav, P. P. (2025). Impact of cold-plasma on the nutritional, textural and structural properties of soy and pea protein isolate for the development of plant-based noodles. *J. Food Sci. Technol.* 1–11.
4. Wang, Y. et al. Effect of high intensity ultrasound on physicochemical, interfacial and gel properties of chickpea protein isolate. *LWT* **129**, 109563 (2020).
5. Rout, S. & Srivastav, P. P. Effect of cold plasma on the technological and functional modification of plant proteins and enzymes. *Innov. Food Sci. Emerg. Technol.* **88**, 103447 (2023).
6. Rout, S. & Srivastav, P. P. Modification of soy protein isolate and pea protein isolate by high voltage dielectric barrier discharge (DBD) atmospheric cold plasma: Comparative study on structural, rheological and techno-functional characteristics. *Food Chem.* **447**, 138914 (2024).
7. Bai, R. et al. Mechanistic study of ultrasound synergy with soybean 11S globulin to improve myofibrillar protein gel properties in low-salt lamb: molecular conformation and water migration. *Food Res. Int.* **211**, 116446 (2025).
8. Zheng, T. et al. Effect of high intensity ultrasound on the structure and physicochemical properties of soy protein isolates produced by different denaturation methods. *Food Hydrocoll.* **97**, 105216 (2019).
9. Shi, R. et al. Combination of high-pressure homogenization and ultrasound improves physiochemical, interfacial and gelation properties of whey protein isolate. *Innov. Food Sci. Emerg. Technol.* **65**, 102450 (2020).
10. Ye, Z., Wang, J., Ma, G. & Ma, J. Ultrasound and glycosylation modifications enhance the physicochemical and functional properties of canola protein isolate for O/W emulsion stabilization. *Food Chem.: X* **28**, 102535 (2025).
11. Peyrano, F., de Lamballerie, M., Avanza, M. V. & Speroni, F. Gelation of cowpea proteins induced by high hydrostatic pressure. *Food Hydrocoll.* **111**, 106191 (2021).
12. Gül, O. et al. Effects of high hydrostatic pressure treatment on structural, techno-functional and rheological properties of sesame protein isolate. *Food Hydrocoll.* **168**, 111549 (2025).
13. Yu, X. X. et al. Study on potential antigenicity and functional properties of whey protein treated by high hydrostatic pressure based on structural analysis. *Food Res. Int.* **173**, 113218 (2023).
14. Yildiz, G. Effects of high-intensity ultrasound, high-pressure processing, and their combination with pH-shifting on the techno-functionality and digestibility of melon seed protein isolate. *Food Res. Int.* **208**, 116219 (2025).
15. Qin, N., Shuang, Q. & Bao, X. High-pressure processing-assisted limited enzymatic hydrolysis improves the luminosity, functional properties, and digestibility of sunflower meal protein. *LWT* **227**, 117989 (2025).
16. Mao, Y. et al. Transglutaminase-induced soybean protein isolate cold-set gels treated with combination of ultrasound and high pressure: Physicochemical properties and structural characterization. *Int. J. Biol. Macromol.* **253**, 127525 (2023).
17. Mao, Y. et al. Riboflavin-loaded soy protein isolate cold gel treated with combination of high intensity ultrasound and high hydrostatic pressure: Gel structure, physicochemical properties and gastrointestinal digestion fate. *Ultrason. Sonochem.* **104**, 106819 (2024).
18. Jiang, L. et al. Effects of ultrasound on the structure and physical properties of black bean protein isolates. *Food Res. Int.* **62**, 595–601 (2014).
19. Chao, D., Jung, S. & Aluko, R. E. Physicochemical and functional properties of high pressure-treated isolated pea protein. *Innov. Food Sci. Emerg. Technol.* **45**, 179–185 (2018).
20. Ahmed, J., Al-Ruwaih, N., Mulla, M. & Rahman, M. H. Effect of high pressure treatment on functional, rheological and structural properties of kidney bean protein isolate. *LWT* **91**, 191–197 (2018).
21. Xu, Y. et al. Effects of ultrasound-assisted punicalagin binding on the allergenicity reduction of soybean protein 7S. *Food Chem.* **482**, 144195 (2025).

22. Zhao, C. et al. Structural characteristics and acid-induced emulsion gel properties of heated soy protein isolate–soy oligosaccharide glycation conjugates. *Food Hydrocoll.* **137**, 108408 (2023).
23. Wang, T. et al. Effect of ultrasound on the preparation of soy protein isolate-maltodextrin embedded hemp seed oil microcapsules and the establishment of oxidation kinetics models. *Ultrason. Sonochem.* **77**, 105700 (2021).
24. Chu, Z. et al. Effect of ultrasound on heated soybean isolate protein-soybean oligosaccharide glycation conjugate acid-induced emulsion gels and their applications as carriers of zeaxanthin. *Food Hydrocoll.* **150**, 109719 (2024).
25. Qu, W. et al. Structure and functional characteristics of rapeseed protein isolate-dextran conjugates. *Food Hydrocoll.* **82**, 329–337 (2018).
26. Zhao, C. et al. Synergistic influence of ultrasound and dietary fiber addition on transglutaminase-induced peanut protein gel and its application for encapsulation of lutein. *Food Hydrocoll.* **137**, 108374 (2023).
27. Qi, Q. et al. Fabrication and characterization of curcumin-loaded complex acid-induced cold gels of soybean and red bean protein isolates incorporated with common and waxy corn starches. *Food Hydrocoll.* **151**, 109863 (2024).
28. Pirestani, S., Nasirpour, A., Keramat, J., Desobry, S. & Jasniewski, J. Structural properties of canola protein isolate-gum Arabic Maillard conjugate in an aqueous model system. *Food Hydrocoll.* **79**, 228–234 (2018).
29. Sheng, L., Liu, Q., Dong, W. & Cai, Z. Effect of high intensity ultrasound assisted glycosylation on the gel properties of ovalbumin: Texture, rheology, water state and microstructure. *Food Chem.* **372**, 131215 (2022).
30. Dev, M. J., Pandit, A. B. & Singhal, R. S. Ultrasound assisted *vis-à-vis* classical heating for the conjugation of whey protein isolate-gellan gum: Process optimization, structural characterization and physico-functional evaluation. *Innov. Food Sci. Emerg. Technol.* **72**, 102724 (2021).
31. Wu, W., Li, F. & Wu, X. Effects of rice bran rancidity on oxidation, structural characteristics and interfacial properties of rice bran globulin. *Food Hydrocoll.* **110**, 106123 (2021).
32. Hu, N. et al. Effect of endogenous protein on starch before and after post-harvest ripening of corn: Structure, pasting, rheological and digestive properties. *Food Chem.* **473**, 143039 (2025).
33. Yan, J. et al. Effect of non-covalent and covalent complexation on structure, functional properties and digestive behavior of soybean protein isolate-soybean isoflavone complexes. *Innov. Food Sci. Emerg. Technol.* **100**, 103928 (2025).
34. Wang, R., Su, C., Li, D. & Wang, L. Effects of inducing conditions on emulsion gel properties of peanut protein isolation-cellulose nanofiber: As extrusion-based 3D food printing inks. *Food Chem.* **495**, 146512 (2025).
35. Shi, A. et al. Effects of proteolysis and transglutaminase crosslinking of physicochemical characteristics of walnut protein isolate. *LWT* **97**, 662–667 (2018).
36. Ren, C. et al. Heat-induced gelation of SAM myofibrillar proteins as affected by ionic strength, heating time and temperature: With emphasis on protein denaturation and conformational changes. *Food Biosci.* **56**, 103320 (2023).
37. Liang, X. et al. Structure, rheology and functionality of whey protein emulsion gels: Effects of double cross-linking with transglutaminase and calcium ions. *Food Hydrocoll.* **102**, 105509 (2020).
38. Wang, X., Han, R., Ramaswamy, H., Wang, C. & Duan, H. Effects of high-pressure processing on physicochemical, structural and emulsifying properties of chicken myofibrillar proteins. *LWT* **229**, 118168 (2025).
39. Zhang, X. et al. Effects of ultrasound combined with pH shift modification on functional and structural properties of peanut proteins. *Int. J. Biol. Macromol.* **283**, 137874 (2024).
40. Tan, M. et al. Effects of combined high hydrostatic pressure and pH-shifting pretreatment on the structure and emulsifying properties of soy protein isolates. *J. Food Eng.* **306**, 110622 (2021).
41. Zou, Y. et al. Effects of different ultrasound power on physicochemical property and functional performance of chicken actomyosin. *Int. J. Biol. Macromol.* **113**, 640–647 (2018).
42. Wang, F. et al. Structural, physicochemical and digestive properties of non-covalent and covalent complexes of ultrasound treated soybean protein isolate with soybean isoflavone. *Food Res. Int.* **189**, 114571 (2024).
43. Huang, D. et al. Effect of combined pH-Shifting and high-intensity ultrasound treatment on the structural, functional, and foaming properties of Tenebrio Molitor Protein. *Food Hydrocoll.* **167**, 111384 (2025).
44. Fu, K. et al. Ultrasound regulates pea protein fibrillation: Impact on aggregation kinetics, physicochemical properties, structure and morphology. *Food Hydrocoll.* **169**, 111609 (2025).
45. Zhang, P. et al. Effect of high intensity ultrasound on transglutaminase-catalyzed soy protein isolate cold set gel. *Ultrason. Sonochem.* **29**, 380–387 (2016).
46. Xue, S. et al. Effects of high-intensity ultrasound, high-pressure processing, and highpressure homogenization on the physicochemical and functional properties of myofibrillar proteins. *Innov. Food Sci. Emerg. Technol.* **45**, 354–360 (2018).
47. Zhao, X. et al. Modifying the physicochemical properties, solubility and foaming capacity of milk proteins by ultrasound-assisted alkaline pH-shifting treatment. *Ultrason. Sonochem.* **88**, 106089 (2022).
48. Wang, Q. et al. Enhancement of foaming performance of hempseed protein by limited enzymatic hydrolysis: From the viewpoint of the structural and interfacial rheological attributes. *Food Chem.* **465**, 142182 (2025).
49. Sun, Y. et al. Effect of power ultrasound pre-treatment on the physical and functional properties of reconstituted milk protein concentrate. *J. Food Eng.* **124**, 11–18 (2014).
50. Zhou, M. et al. Effect of high intensity ultrasound on physicochemical and functional properties of soybean glycinin at different ionic strengths. *Innov. Food Sci. Emerg. Technol.* **34**, 205–213 (2016).
51. Dehnad, D., Emadzadeh, B., Ghorani, B. & Rajabzadeh, G. High hydrostatic pressure (HHP) as a green technology opens up a new possibility for the fabrication of electrospun nanofibers: Part I - improvement of soy protein isolate properties by HHP. *Food Hydrocoll.* **140**, 108659 (2023).
52. Li, D. et al. Effects of (+)-catechin on a rice bran protein oil-in-water emulsion: Droplet size, zeta-potential, emulsifying properties, and rheological behavior. *Food Hydrocoll.* **98**, 105306 (2020).
53. Zhao, C. et al. Ultrasound-induced red bean protein–lutein interactions and their effects on physicochemical properties, antioxidant activities and digestion behaviors of complexes. *LWT* **160**, 113322 (2022).
54. Hegde, K. R. et al. Effects of ultrasound and high-pressure assisted extraction of pearl millet protein isolate: Functional, digestibility, and structural properties. *Int. J. Biol. Macromol.* **289**, 138877 (2025).
55. Yang, J. et al. Application of edible insects to food products: A review on the functionality, bioactivity and digestibility of insect proteins under high-pressure/ultrasound processing. *Food Chem.* **468**, 142469 (2025).
56. McLauchlan, J., Tyler, A. I. I., Chakrabarti, B., Orfila, C. & Sarkar, A. Oat protein: Review of structure-function synergies with other plant proteins. *Food Hydrocoll.* **154**, 110139 (2024).
57. Hu, N. et al. Postharvest ripening of newly harvested corn: Weakened interactions between starch and protein. *Food Chem.* **451**, 139450 (2024).
58. Zhao, C. et al. Structure and acid-induced gelation properties of soy protein isolate–maltodextrin glycation conjugates with ultrasonic pretreatment. *Food Hydrocoll.* **112**, 106278 (2021).

59. Zhao, C. et al. Interactions of soy protein isolate with common and waxy corn starches and their effects on acid-induced cold gelation properties of complexes. *Food Chem.: X* **18**, 100671 (2023).
60. Tian, Y. et al. Interaction between pH-shifted β-conglycinin and flavonoids hesperetin/hesperidin: Characterization of nanocomplexes and binding mechanism. *LWT* **140**, 110698 (2021).
61. Zhao, C. et al. Improvement of structural characteristics and in vitro digestion properties of zein by controlling postharvest ripening process of corn. *Food Control* **142**, 109221 (2022).
62. Cortés-Ríos, J. et al. Protein quantification by bicinchoninic acid (BCA) assay follows complex kinetics and can be performed at short incubation times. *Anal. Biochem.* **608**, 113904 (2020).
63. Qi, Q. et al. Effects of two types of corn starches on physicochemical and structural properties of red bean protein isolate acid-induced cold gels. *J. Food Eng.* **381**, 112187 (2024).

Acknowledgements

This work was supported by the Science and Technology Development Program of Jilin Province of China (No. 20250202019NC), the Open Project Program of National Engineering Research Center of Wheat and Corn Further Processing, Henan University of Technology (No. NL2024015), and the China Agriculture Research System (No. CARS-02).

Author contributions

J.L.: Methodology, Writing – original draft. J.Y.: Data curation, Formal analysis. F.X.: Software, Visualization. J.W.: Project administration. Q.F.: Resources. Q.G.: Investigation, Resources. J.G.: Project administration, Supervision. C.Z.: Conceptualization, Writing – review & editing. J.L.: Funding acquisition, Validation.

Competing interests

The authors declare no competing interests.

Additional information

Supplementary information The online version contains supplementary material available at https://doi.org/10.1038/s41538-025-00662-x.

Correspondence and requests for materials should be addressed to Jiannan Yan, Chengbin Zhao or Jingsheng Liu.